

# Particle size effect on the crystal structure symmetry of $K_{0.5}Na_{0.5}NbO_3$

Yosuke Shiratori<sup>\*</sup>, Arnaud Magrez<sup>1</sup>, Christian Pithan

*Institut für Elektronische Materialien, Institut für Festkörperforschung (IFF), Forschungszentrum Jülich GmbH, D-52425 Jülich, Germany*

Available online 12 April 2005

## Abstract

Pure sodium potassium niobates with  $K_{0.5}Na_{0.5}NbO_3$  composition were prepared in powderous form with various particle sizes (75 nm–10  $\mu$ m) through microemulsion mediated synthesis and subsequent annealing. An interesting change of particle shape and a mixture of fine and coarse particles were observed at a critical diameter of 200 nm. A combined study by X-ray powder diffraction (XRPD) and Raman spectroscopy demonstrated a phase transformation induced by particle size. Fine particles (<200 nm) have a triclinic structure whereas coarse particles (>200 nm) have a monoclinic structure at room temperature. Possible space groups describing both these modifications were suggested. © 2005 Elsevier Ltd. All rights reserved.

*Keywords:* Powders-chemical preparation; X-ray methods; Niobates; Perovskites; Raman spectroscopy

## 1. Introduction

Ferroelectric properties of nanocrystalline transition metal-based oxide particles do not only depend on intrinsic parameters, as for instance stoichiometry or overall chemical composition but are also strongly determined by the particle size of the powder.<sup>1</sup> Alkaline niobates such as  $K_xNa_{1-x}NbO_3$  are considered to be a promising class of lead free piezoelectric materials representing an environment-friendly alternative to  $Pb(Zr, Ti)O_3$ , which typically contains more than 60 wt.% lead.<sup>2</sup> However, their sintering behavior is rather poor. Therefore, nanocrystalline powders of these niobates are needed to improve the sinterability and in order to prepare dense piezoceramics. The crystal structure of such nanocrystalline product is of importance because it is correlated with most of their materials properties, such as mechanical strength, toughness, ferroelectricity and piezoelectric response.

Here we focus on  $K_{0.5}Na_{0.5}NbO_3$  as a technically interesting composition<sup>3</sup> and investigate the size effect on the crystallographic phase transformation.<sup>4</sup> Since we only

can determine the Laue classes from diffraction patterns and because of the broadening of Bragg reflections caused by the small particle size of the powders, conventional X-ray diffraction sets limitations in understanding the real crystal structure. Therefore we combine X-ray powder diffraction (XRPD) and Raman spectroscopy, which is very sensitive to phase transitions,<sup>5,6</sup> in order to acquire additional evidence for the true crystallographic structure in  $K_{0.5}Na_{0.5}NbO_3$  nanoparticles.

## 2. Experimental procedure

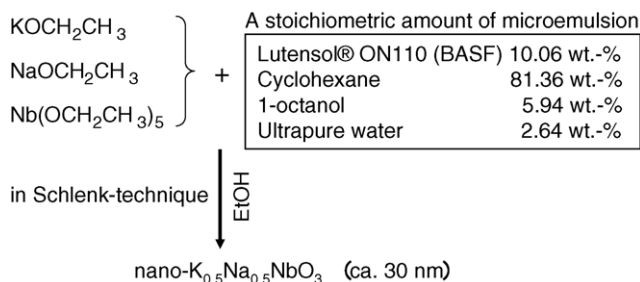
Mixed alkoxide solutions prepared from the respective pure alkali metal ethoxides and pure niobium ethoxides in ethanol were hydrolyzed by the addition of a water/oil microemulsion. The principle of the synthesis route has been described by Herrig and Hempelmann.<sup>7</sup> The aqueous micelles serve as templates or nanoreactors and therefore particle nucleation and growth can be controlled during particle formation. The outline of the process used in this work is shown in *Scheme 1*. The details are reported in elsewhere.<sup>8</sup>

After precipitation of the raw powders, calcination treatments at temperatures between 200 and 1000 °C were performed in air for 1 h, respectively. This yielded in annealed powders with a large variation in particle size ranging from

<sup>\*</sup> Corresponding author. Tel.: +49 2461 614389; fax: +49 2461 612550.

*E-mail address:* [yo.shiratori@fz-juelich.de](mailto:yo.shiratori@fz-juelich.de) (Y. Shiratori).

<sup>1</sup> Present address: Laboratoire des Nanostructures et des Nouveaux Matériaux Électroniques (LNNME), École Polytechnique Fédérale de Lausanne (EPFL), CH-1015 Lausanne-EPFL, Switzerland.



Scheme 1. Synthetic scheme for nano- $\text{K}_{0.5}\text{Na}_{0.5}\text{NbO}_3$  powders prepared in this work.

about 75 nm to 10  $\mu\text{m}$ . These values of the average particle size were determined using FE-SEM (Carl Zeiss LEO1530) and by measuring the mean free powder surface by  $\text{N}_2$ -adsorption (BET method, Micromeritics Gemini 2360). From this free powder surfaces, the BET equivalent particle diameter was estimated assuming a spherical morphology and a theoretical density of  $4.51 \text{ g/cm}^3$ . Inductively coupled plasma with optical emission spectroscopy showed that the stoichiometry did not change over the range of the annealing temperature applied.

X-ray powder diffraction (XRPD) patterns of the prepared powders were measured at room temperature in Debye–Scherrer geometry using a Philips X'Pert diffractometer with  $\text{Cu K}\alpha$  radiation. Structure refinements were carried out by full pattern matching refinement using the program FULLPROF.

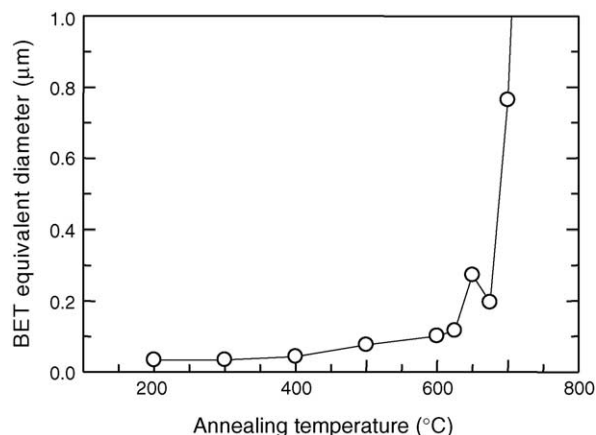


Fig. 1. Annealing temperature dependence of BET equivalent  $\text{K}_{0.5}\text{Na}_{0.5}\text{NbO}_3$  particle diameter.

Raman spectra were recorded for these powders at various temperatures using a Jobin Yvon T64000 spectrometer. An  $\text{Ar}^+$  laser with 514.5 nm wavelength and  $<50 \text{ mW}$  power at the samples (BeamLok 2080, Spectra-Physics) was used for sample excitation. Powder samples of ca. 10 mg were mounted on a quartz crucible. This crucible was covered by a glass slide and placed on a silver heating block of the THMS600 stage (Linkam Scientific Co.) with a temperature accuracy better than  $0.1 \text{ }^\circ\text{C}$ . Curve analysis for the obtained spectra was performed using a program included in the Grams/AI software (Thermo Galactic).

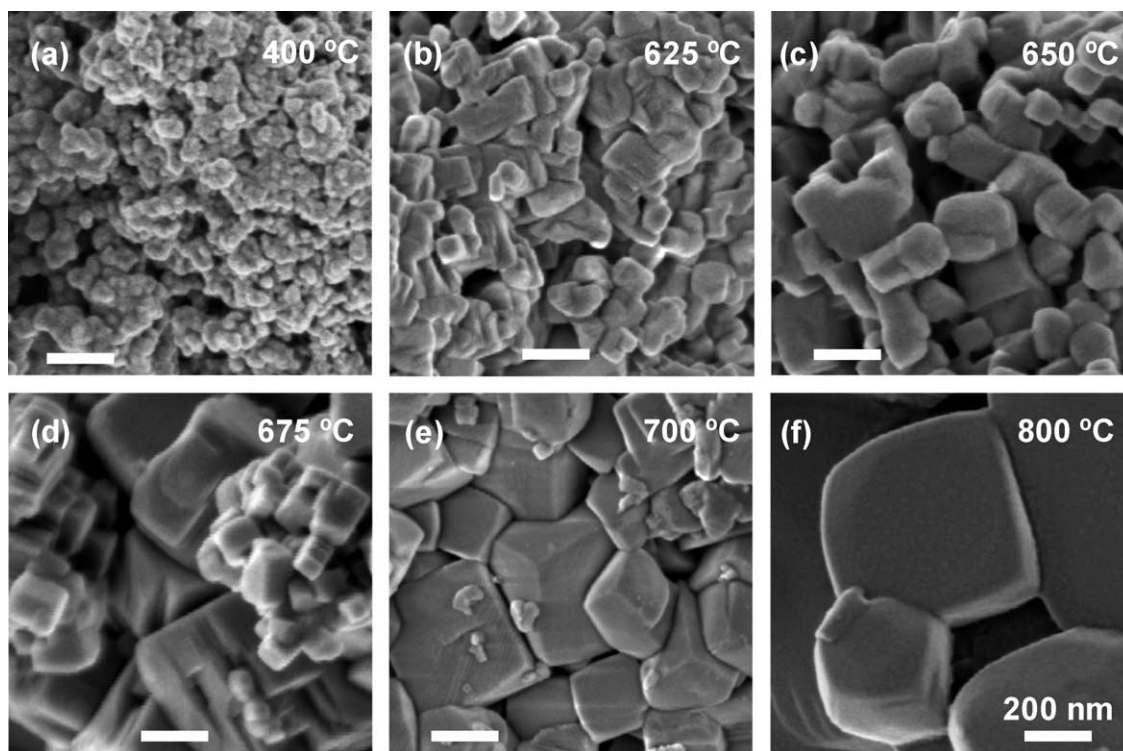


Fig. 2. SEM images of  $\text{K}_{0.5}\text{Na}_{0.5}\text{NbO}_3$  powders annealed for 1 h at  $400 \text{ }^\circ\text{C}$  (a),  $625 \text{ }^\circ\text{C}$  (b),  $650 \text{ }^\circ\text{C}$  (c),  $675 \text{ }^\circ\text{C}$  (d),  $700 \text{ }^\circ\text{C}$  (e) and  $800 \text{ }^\circ\text{C}$  (f).

Fluorescence background as well as Raman bands originating from the carbon-chain deformation modes, the C–O and C–C stretching modes<sup>9</sup> were observed in the Raman spectra for powders annealed up to 400 °C. Above 500 °C, no evidence for organic contamination could be detected by Raman spectroscopy.

### 3. Results and discussion

The dependence of particle diameter from annealing temperature obtained through BET adsorption measurements is shown in Fig. 1. Obviously particle growth started at 400 °C. The temperature characteristic became steeper above 600 °C and particles grew drastically and coarsened above 700 °C. Selected SEM images of the powders after annealing are shown in Fig. 2. Particles after annealing at 400 °C seem to be still coated with residual surfactant from the microemulsion (Fig. 2a). The diameters of the particles in Fig. 2b and c were <200 and >200 nm, respectively and the powders af-

ter annealing at 650 and 675 °C (Fig. 2c and d) consisted in a mixture of fine (<200 nm) and coarse (>200 nm) particles. XRPD patterns showed that the particles obtained after hydrolysis were amorphous and that a calcination temperature of 500 °C was not sufficient for crystallization. The patterns for the powders obtained after annealing above 600 °C indicated sharp profiles (Fig. 3), i.e. well crystallized powders. The enlarged XRPD patterns for the powders annealed at 625, 650, 675 and 700 °C are also indicated in the order of particle size as insets of Fig. 3. For the fine powder (<200 nm), some additional peaks were detected at 35.92° and 42.82° in 2θ, which are not present in the patterns for the coarse powder (>200 nm). Within the intermediate diagrams, the profiles look as a superimposition of those of the fine and coarse powders. This tendency was also observed in the 65–68° region. As results of full pattern matching refinement, the diffraction pattern of the coarse particles, registered at room temperature, could be indexed with the lattice parameters  $a_M = 4.0045(6)$  Å,  $b_M = 3.9452(2)$  Å,  $c_M = 3.9989(2)$  Å and  $\beta_M = 90.345(2)^\circ$ , corresponding to a

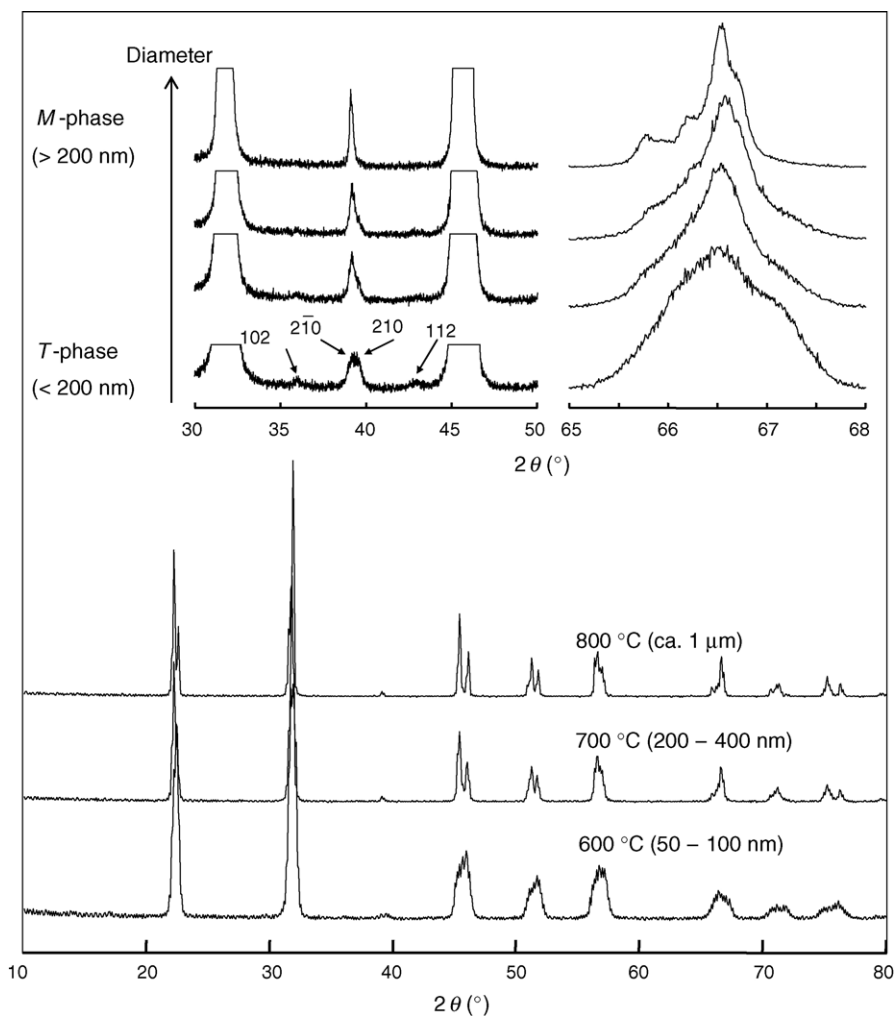


Fig. 3. XRPD patterns for  $K_{0.5}Na_{0.5}NbO_3$  powders annealed at various temperatures for 1 h. Particle sizes are indicated in parentheses. Enlarged XRPD patterns for the powders annealed for 1 h at 625, 650, 675 and 700 °C are indicated in order of particle size as the inset of the graph.

monoclinic cell (one perovskite formula ( $Z=1$ ) per unit cell). Isotypic phases, with this M-type structure, were reported in the  $\text{KNbO}_3\text{--NaNbO}_3$  binary system.<sup>10</sup> Based on the XRD extinction rules, three different space groups are possible for the M-type structure:  $P2/m$  ( $C_{2h}^1$ ),  $P2$  ( $C_2^1$ ) and  $Pm$  ( $C_s^1$ ). The room temperature diffraction pattern of the fine particles was refined with a triclinic lattice (T-type structure), with  $a_T=5.6696(6)$  Å,  $b_T=3.9391(2)$  Å,  $c_T=5.5982(3)$  Å,  $\alpha_T=89.837(6)^\circ$ ,  $\beta_T=90.670(2)^\circ$  and  $\gamma_T=90.273(6)^\circ$ , i.e.  $Z=2$ . Two space groups are possible for the description of the T-type structure:  $P1$  ( $C_1^1$ ) or  $P-1$  ( $C_i^1$ ).

Fig. 4 shows Raman spectra measured at various temperatures for the fine, intermediate and coarse powders. The  $\nu_1$  to  $\nu_6$  modes are internal vibrational modes of  $\text{NbO}_6$  octahedra under the equilateral shape approximation<sup>6,11</sup> and the bands at  $<160\text{ cm}^{-1}$  seem to be assigned to the  $\text{Na}^+/\text{K}^+$  translational mode and the rotation of the  $\text{NbO}_6$  octahedra.<sup>6</sup> Since the space group  $P2/m$  has no Raman active modes based on the nuclear site group analysis,<sup>12</sup> only the  $P2$  and  $Pm$  groups with Raman active normal modes,  $4A+8B$  and  $8A'+4A''$ , respectively, are considered as possible. The Raman active normal modes for both T-type polymorphs ( $P1$  ( $C_1^1$ ) and  $P-1$  ( $C_i^1$ )) are represented as  $27A$  and  $6A_g$ , respectively, however the curve fitting by a combination of Lorentzian and Gaussian functions for the T-type spectrum which was obtained at room temperature indicated the existence of more than 16 bands in this raw spectrum. Therefore,  $P1$  is the more suitable polymorph for T-type structure at room temperature. The spectrum for T-type structure in this report was significantly different from that for M-type (see the dotted lines in Fig. 4a and c). Especially, band broadening of the degenerated modes ( $\nu_2$  ( $E_g$ ),  $\nu_5$  ( $F_{2g}$ ),  $\nu_1+\nu_5$  ( $A_{1g}\times F_{2g}=F_{2g}$ )) under the equilateral  $\text{NbO}_6$  octahedron approximation were observed in the T-type spectrum (Fig. 4a). Site symmetries of the octahedra in a crystal field and dynamic coupling of the internal modes of octahedra<sup>13</sup> cause the splitting of such degenerated modes.

On the temperature turning measurements, clear alterations of the spectrum were observed at about 220 and 430 °C for the coarse powder (Fig. 4c). These values are close to the phase transition temperatures of  $\text{K}_{0.5}\text{Na}_{0.5}\text{NbO}_3$  ceramic reported in literature.<sup>3,10</sup> For the fine powder (Fig. 4a), the temperature interval on such spectral transition was much wider similar to the case of the tetragonal to cubic transition of nano- $\text{BaTiO}_3$  particles which was related to a distribution in tetragonality.<sup>5</sup> In Fig. 4a, the  $\nu_1+\nu_5$  mode is retained up to 500 °C. This result indicates significant distortions in the  $\text{NbO}_6$  octahedra from a perfect one or the existence of different crystal field effects on each octahedron at such high temperature.

The perovskite formula volumes ( $V_{\text{unit cell}}/Z$ ) were calculated from lattice parameters as 63.18(1) and 62.50(1) Å<sup>3</sup> for both T- and M-structures, respectively. Generally, a decrease in crystal size accompanies an increase in surface tension and this leads to a decrease of lattice parameters or a transformation of crystallographic structure toward a more symmetric one.<sup>5</sup> However, nano- $\text{K}_{0.5}\text{Na}_{0.5}\text{NbO}_3$  powders

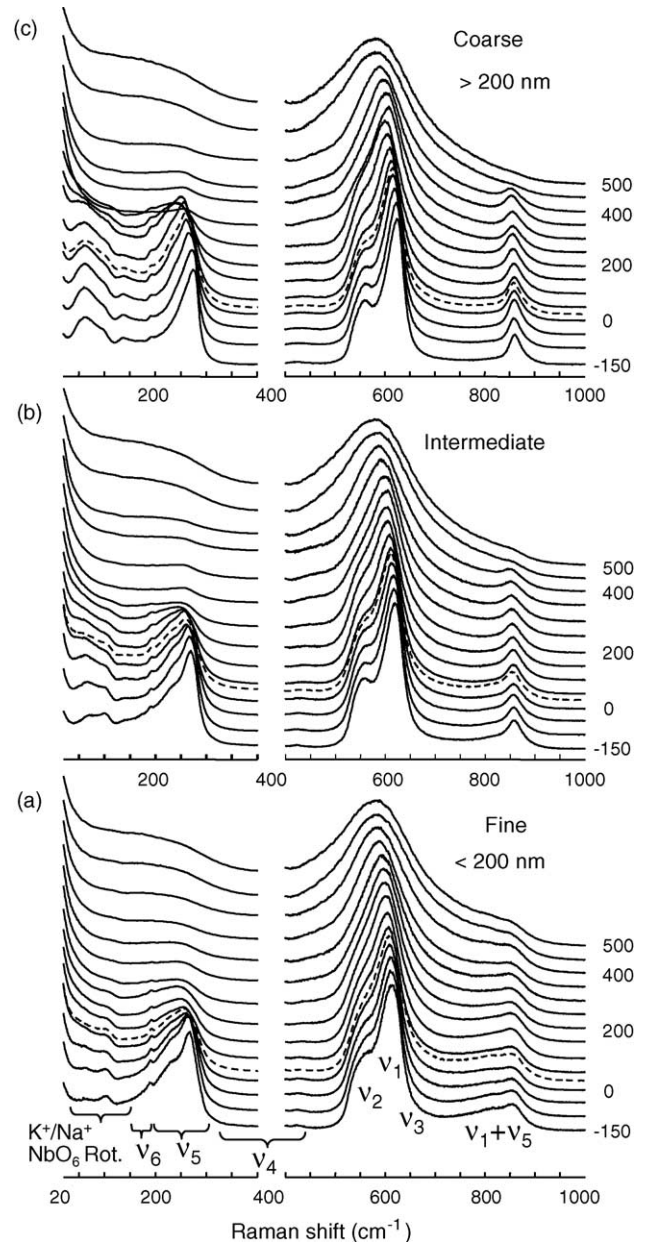


Fig. 4. Raman spectra of the fine (a), intermediate (b) and coarse (c) powders recorded at various temperatures ( $\Delta T=50$  °C). Some temperatures in °C are indicated in the right side of the spectra. The spectra measured at room temperature are shown by using dotted lines.

presented in this report indicated an opposite behavior, from the monoclinic phase to less symmetric triclinic phase. Na/K atomic distribution and also charge distribution<sup>14</sup> in the lattice should be discussed as a possible origin for this phase transformation.

#### 4. Conclusion

Pure  $\text{K}_{0.5}\text{Na}_{0.5}\text{NbO}_3$  powders with a range of particle size from 75 nm to roughly 10  $\mu\text{m}$  were prepared through

microemulsion-mediated synthesis followed by annealing. The thermodynamically stable structure at room temperature, monoclinic (M-type:  $P2$  or  $Pm$ ), was refined for the coarse particles ( $>200$  nm), while for the finer particles ( $<200$  nm) a new metastable triclinic polymorph (T-type) was found.  $P1$  was considered to be more consistent space group than  $P-1$  for the T-type structure.

### Acknowledgements

We would like to acknowledge Dr. J. Dornseiffer and Dr. F.-H. Haegel for support in powder synthesis, Dr. E. Wessel for SEM studies and Dr. W. Krasser and Dr. W. Sager for fruitful discussions. One of the authors (Y. Shiratori) gratefully acknowledges the Alexander von Humboldt Foundation (Bonn, Germany) for granting financial support through a Research Fellowship.

### References

1. McNeal, M. P., Jang, S.-J. and Newnham, R. E., The effect of grain and particle size on the microwave properties of barium titanate ( $\text{BaTiO}_3$ ). *J. Appl. Phys.*, 1998, **83**, 3288–3297.
2. Ringgaard, E. and Wurlitzer, T., Lead-free piezoceramics based on alkali niobates. In *Electroceramics IX*, 2004 (C7-507).
3. Jaffe, B., Cook, W. R. and Jaffe, H., *Piezoelectric Ceramics*. Academic Press, London, 1971, pp. 185–212.
4. Shiratori, Y., Magrez, A. and Pithan, C., Phase transformation of  $\text{KNaNb}_2\text{O}_6$  induced by size effect. *Chem. Phys. Lett.*, 2004, **391**, 288–292.
5. Begg, B. D., Finnie, K. S. and Vance, E. R., Raman study of the relationship between room-temperature tetragonality and the Curie point of barium titanate. *J. Am. Ceram. Soc.*, 1996, **79**, 2666–2672.
6. Shen, Z. X., Wang, X. B., Kuok, M. H. and Tang, S. H., Raman scattering investigations of the antiferroelectric–ferroelectric phase transition of  $\text{NaNbO}_3$ . *J. Raman Spectrosc.*, 1998, **29**, 379–384.
7. Herrig, H. and Hempelmann, R., A colloidal approach to nanometre-sized oxide ceramics powders. *Mater. Lett.*, 1996, **27**, 287–292.
8. Pithan, C., Shiratori, Y., Dornseiffer, J., Haegel, F.-H., Magrez, A. and Waser, R., Microemulsion mediated synthesis of nanocrystalline  $(\text{K}_x\text{Na}_{1-x})\text{NbO}_3$  powders. *J. Cryst. Growth*, 2005, in press.
9. Barańska, H., Łabudzińska, A. and Terpiński, J., *Laser Raman Spectrometry: Analytical Applications*. Ellis Horwood Limited, Chichester, 1987, Chapter 4, pp. 94, 117.
10. Ahtee, M. and Hewat, A. W., Structural phase transition in sodium-potassium niobate solid solutions by neutron powder diffraction. *Acta Cryst.*, 1978, **A34**, 309–317.
11. Herzberg, G., *Molecular Spectra and Molecular Structure: II. Infrared and Raman Spectra of Polyatomic Molecules*. Van Nostrand, New York, 1945, p. 122.
12. Rousseau, D. L., Bauman, R. P. and Porto, S. P. S., Normal mode determination in crystals. *J. Raman Spectrosc.*, 1981, **10**, 253–290.
13. Poulet, H. and Mathieu, J. P., *Vibration Spectra and Symmetry of Crystals*. Gordon and Breach, New York, 1976, Chapter 5.
14. Gamarnik, M. Ya., Tensile and compressive effect of intracrystalline pressure in small particles. *Phys. Stat. Sol. (b)*, 1991, **164**, 107–119.